Fluorescence of unmodified oligonucleotides: A tool to probe G-quadruplex DNA structure

ARTICLE *in* BIOPOLYMERS · OCTOBER 2009

Impact Factor: 2.39 · DOI: 10.1002/bip.21268 · Source: PubMed

2 AUTHORS:

Miguel Méndez
Universidad San Francisco de Quito (USFQ)
17 PUBLICATIONS **76** CITATIONS
SEE PROFILE

Veronika A Szalai
National Institute of Standards and Technology
42 PUBLICATIONS **1,581** CITATIONS
SEE PROFILE

Fluorescence of Unmodified Oligonucleotides: A Tool to Probe G-Quadruplex DNA Structure

Miguel Angel Mendez, Veronika A. Szalai
Department of Chemistry and Biochemistry, University of Maryland, Baltimore County, Baltimore, MD 21250

Received 20 February 2009; revised 12 June 2009; accepted 13 June 2009
Published online 22 June 2009 in Wiley InterScience (www.interscience.wiley.com). DOI 10.1002/bip.21268

ABSTRACT:

Fluorescence of unmodified oligonucleotides has not been exploited for guanine-quadruplex (G-quadruplex) characterization. We observe that G-rich sequences fluoresce more strongly than duplex or single-stranded DNA but much more weakly than fluorophores like fluorescein. This increase in the intrinsic fluorescence is not due to an increase in absorption at the excitation wavelength but rather to a change in the quantum yield. We show that unlabeled oligonucleotides that form G-quadruplexes can be differentiated on the basis of their emission spectra from similar sequences that do not contain consecutive guanines. Intermolecular quadruplexes formed by the oligonucleotides 5′-$T_4G_nT_4$-3′ ($n = 4$–10) display a nonlinear, but continuous, increase in emission intensity as the G content increases. The sequence 5′-GGGT-3′, which has been proposed to form a monomeric quadruplex and an interlocked quadruplex (Krishnan-Ghosh et al. J Am Chem Soc *2004, 126, 11009), was compared with the similar sequence 5′-TGGG-3′, the structure of which has not been characterized. Both the maximum emission intensity and the spectral shape differ for these oligonucleotides as a function of sample preparation, indicating that different types of quadruplexes form for both sequences. Our work is the first to demonstrate that the suprastructure of G-rich sequences can be probed using fluorescence signatures of unmodified oligonucleotides.* © *2009 Wiley Periodicals, Inc. Biopolymers 91: 841–850, 2009.*

Keywords: *guanine; quadruplex; fluorescence; exciplex*

This article was originally published online as an accepted preprint. The "Published Online" date corresponds to the preprint version. You can request a copy of the preprint by emailing the Biopolymers editorial office at biopolymers@wiley.com

INTRODUCTION

Molecules of DNA rich in guanine present significantly higher fluorescence than homologous chains without consecutive guanines (G).[1] To demonstrate the usefulness of this electronic property, we have studied several sequences capable of forming a particular superstructure known as a guanine-quadruplex (G-quadruplex, Scheme 1). G-quadruplexes, four stranded structures mediated by hydrogen-bonded Gs (Scheme 1), have been implicated in gene control and other biological processes.[2,3] They are used as drugs for treating cancer[4] and as sources for new materials.[5–7] Use of fluorescently modified DNA, either labeled with extrinsic fluorophores[8] or intrinsic fluorescence enhanced by metallic particles,[9] is a common means to detect and monitor the structure, hybridization, and binding properties of DNA. These technologies have enabled the creation of broadly used tools such as molecular beacons, DNA chips, and aptamer-based fluorescence sensors.[9–14] Fluorescence resonance electron transfer (FRET) in molecular beacons has been exploited in the detection of folded and unfolded states of oligonucleotides.[15–17] These changes have been coupled with sensing capabilities to detect a variety of analytes. FRET also has been used to detect movements of nanomachines.[5] In some instances, however, addition of a fluorescent tag—often

Additional Supporting Information may be found in the online version of this article.

Correspondence to: V. A. Szalai; e-mail: vszalai@umbc.edu

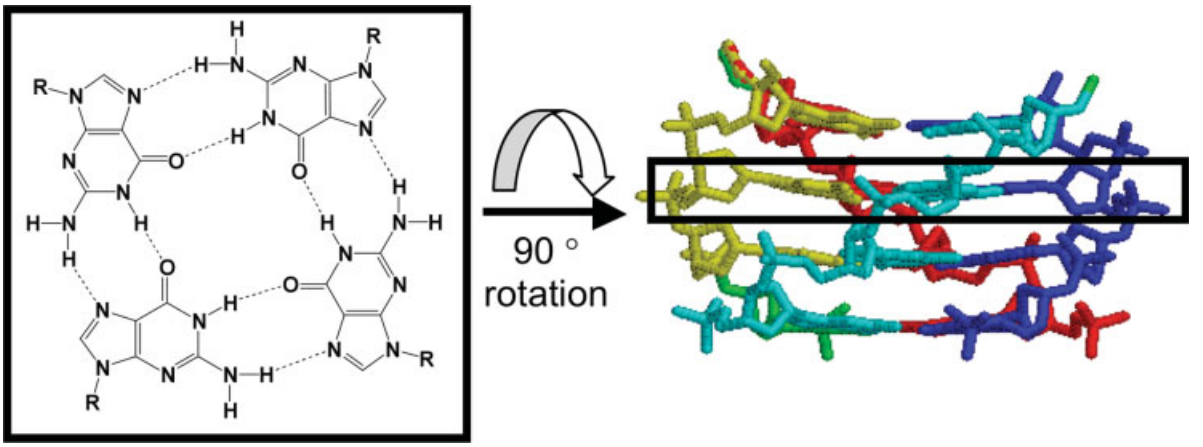

SCHEME 1 Four hydrogen-bonded guanines make a G-quartet plane (left); R is the sugar-phosphate backbone of DNA. Four d(TG_4T) strands (different colors) form a G quadruplex that contains four G-quartet planes (right, pdbid 352D, modified). The G quartet on the left is rotated 90° compared with the boxed G-quartet on the right. Thymines in the structure on the right have been removed for clarity.

a large aromatic molecule or other bulky group—is not desirable. For example, addition of a single 3′T residue to oligonucleotides can interfere with supramolecular assembly of DNA.[18,19] In such cases, monitoring intrinsic DNA fluorescence to probe DNA structure would be advantageous.

Although the intrinsic fluorescence of DNA has not been exploited previously for the characterization of G-quadruplexes, we reasoned that DNA sequences with runs of contiguous guanines should provide sufficient fluorescence signal to monitor DNA structure.[20] Native DNA has a low-quantum yield,[9] on the order of 10^{-4} to 10^{-5} compared with strongly fluorescent dyes like fluorescein 0.95,[21] Cy3 0.04,[22] or tryptophan 0.13.[21] Upper limits for the lowest excited singlet lifetimes are 1 ps for the mononucleotides cytosine and thymine and 10 ps for adenine and guanine.[23] Some DNA polymers have been reported to have excited-state lifetimes of ~100 ps and even upto 1 ns.[14,24,25] The quantum yield of polyG at room temperature in aqueous solution, however, is 4.7×10^{-4}, which makes it the native DNA sequence with the highest intrinsic fluorescence.[1] Excited-states generated by UV-irradiation of short duplexes and hairpins containing GC base pairs have been shown to decay more slowly than their mononucleotide counterparts.[26] The sequence $d(G)_{20}$ has been reported to have the highest average fluorescence lifetime (11.3 ps) out of a series of single-stranded and duplex oligonucleotides probed.[27] On the basis of this information, we demonstrate that emission from unmodified-oligonucleotides can be used to expand our understanding of the structure and properties of polymers rich in G, in particular, G-quadruplexes.

RESULTS

Emission Intensities

Our first step toward the implementation of emission spectroscopy to characterize unmodified G-quadruplexes was evaluation of the feasibility of distinguishing the emission of G-quadruplexes from homologous nonquadruplex forming sequences. Figure 1 shows that the emission intensity of the G4, G7, and G9 oligonucleotides increases as the number of

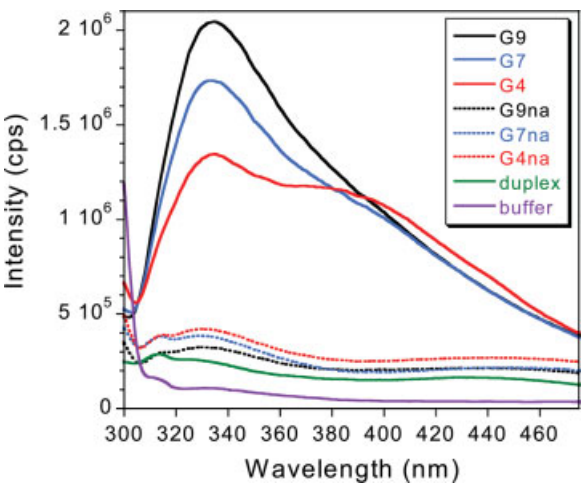

FIGURE 1 Emission spectra of G4, G7, G9, G4na, G7na, G9na, and 9G-1:9G-2 (duplex) in 10 m*M* KPi, 50 m*M* KCl, pH 7.0. The oligonucleotide strand concentration was 30 μM; the duplex concentration also was 30 μM so that the concentration of Gs was matched to the G9 sample. Experiment was performed at room temperature, excitation at 270 nm.

adjacent Gs increases from four to seven to nine. This increase is not due to the total number of guanines in the sequence because the oligonucleotides G4na, G7na, and G9na all have approximately the same emission intensity as one another, even though these oligonucleotides also contain four (G4na), seven (G7na), and nine (G9na) Gs. Note that the emission intensity of these oligonucleotides is four-to-five times lower than the emission intensity of their counterparts with adjacent Gs. The double-stranded DNA (9G-1:9G-2) that contains nine randomly positioned Gs presents even lower emission intensity than the single-stranded sequence with nine Gs. These results encouraged us to proceed with exploiting the observed increased emission intensity as a means to characterize quadruplex structures.

Our next logical step was to explore whether the observed increase in emission intensity was due exclusively to the presence of consecutive Gs in a sequence or the unique environment of these consecutive Gs in a G-quadruplex. We used the oligonucleotides G3T[28] and 4G in the absence and presence of potassium ions to test this idea. The oligonucleotide G3T forms an intermolecular quadruplex.[28] The sequence 4G has not been used previously as a G-quadruplex forming oligonucleotide to the best of our knowledge, but several sequences containing a GGGG repeat have been characterized and they form parallel-stranded intramolecular quadruplexes.[29–32] Note that the oligonucleotides G4, G7, and G9 from Figure 1 are not suitable for testing the idea that quadruplex formation is requisite for enhanced-emission intensity because the single-stranded:quadruplex equilibrium favors quadruplex for these sequences. We have observed that quadruplexes formed by these sequences are very difficult to disrupt by melting or other methods.[33]

The emission intensities of 4G and G3T samples that were heated to 90°C and allowed to cool slowly in the presence of potassium were higher than the emission of matched samples in water that were heated to 90°C and immediately immersed in ice to discourage quadruplex formation (Figures 2A and 3A). Circular dichroism (CD) spectra of these same samples confirmed that quadruplex structures form in buffer containing K^+ (Figures 2B and 3B). For 4G, the CD spectra show that the spectrum collected in potassium buffer presents features consistent with quadruplex formation (maximum at 260 nm and minimum at 238 nm, Figure 2B). Changes in emission intensity for 4G are quite dramatic: an approximately fivefold higher emission signal in potassium-containing buffer than in water (Figure 2A). This oligonucleotide shows the biggest difference in intensity observed in our study thus far. Like 4G, the CD spectrum of G3T adopts a classical parallel-stranded quadruplex signature in the presence of K^+. Also like 4G, the G3T emission spectral intensity

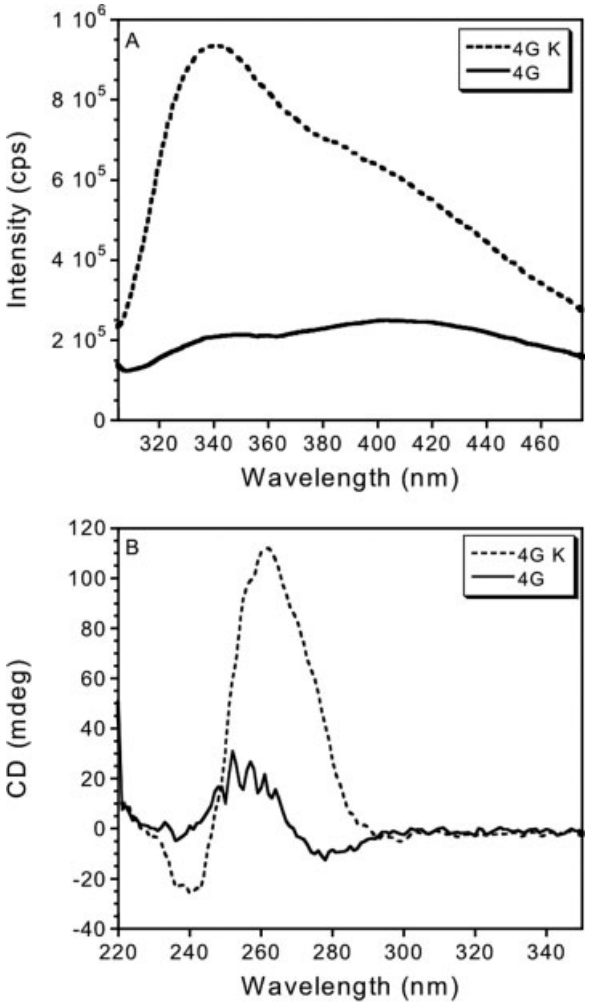

FIGURE 2 (A) Emission spectra of oligonucleotide 4G in the presence (dotted line) and absence (solid line) of potassium ions. Each spectrum is the average of three independent spectra. (B) CD spectra of 4G in the presence (dotted line) and absence (solid line) of potassium ions. The CD sample concentration was 70 μM and the emission sample concentration was 14 μM.

increases in the presence of potassium ions but the increase is not as great (only approximately twofold) as that observed for 4G.

We performed a similar series of experiments (fluorescence and CD spectroscopy) in which one set of samples was suspended in a solution of tetramethylammonium chloride (TMAC) at the same ionic strength and pH as the potassium-containing buffer samples (Supporting Figures S1–S3). The shapes of the CD and fluorescence spectra of 4G, G3T, and TG3 in TMAC (Figures S1–S3) are very similar to those collected in water (Figures 2–4) indicating that quadruplex-forming conditions (i.e., the presence of potassium ions) are required to produce increased fluorescence intensity for these sequences.

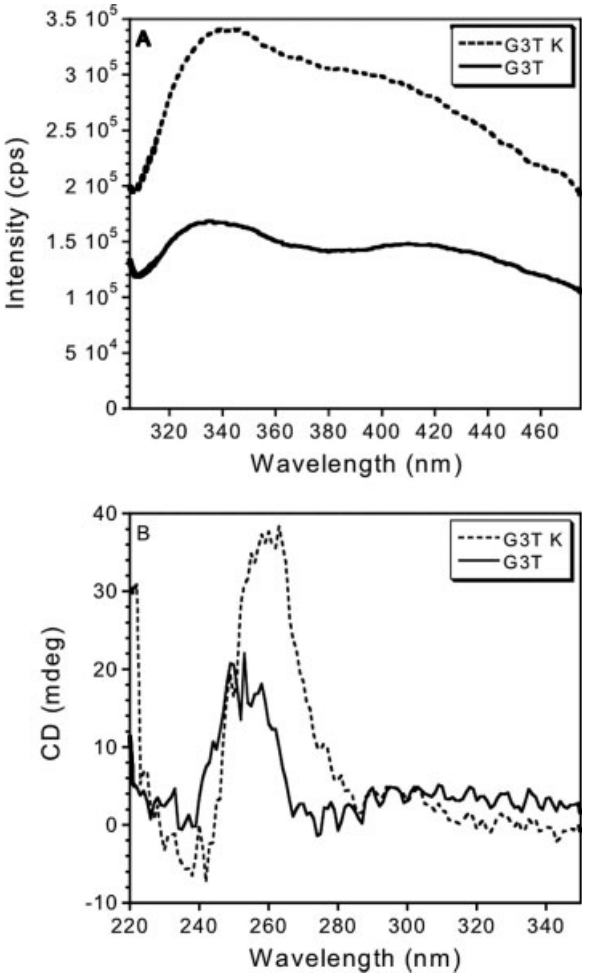

FIGURE 3 (A) Emission spectra of the oligonucleotide G3T in the presence (dotted line) and absence (solid line) of potassium ions. Each spectrum is the average of three independent spectra. (B) CD spectra of G3T in the presence (dotted line) and absence (solid line) of potassium ions. The CD sample concentration was 68 μM and the emission sample concentration was 15 μM.

Quantum Yield

Using G9, the longest quadruplex-forming sequence in our series, an upper limit on the quantum yield of quadruplexes was determined to be 2.39×10^{-4}. This value was obtained by comparison to the standard guanine in water, which was secondarily calibrated to the standard 2,5-diphenyloxazole.[21] Plots of the integrated intensity of the fluorescence vs. absorption required for calculation of the quantum yield are presented in the Supporting Information (Figures S8 and S9).

Using Emission to Probe G-Rich DNA Structures

To develop emission of unmodified quadruplexes as a sensitive structural probe, we next sought to correlate emission, CD, and nondenaturing PAGE of the structurally uncharacterized sequence TG3. The emission spectra of TG3 with or without K^+ are very similar in shape and differ only slightly in intensity (Figure 4) even though CD spectra indicate that the structure has changed (Figure 4B). In fact, the CD spectra of TG3 and G3T in K^+ are very similar in shape and intensity (Figure S4). The emission intensities in TMAC differ for the two sequences, but the spectral shapes are similar (Figure S4). The low signal to noise in the CD spectra, in particular in TMAC, is because short oligonucleotides have low-CD spectral intensities unless they form larger supramolecular structures with extended helicity.[34] The major difference between the two sequences is the emission intensity in the presence of added K^+, which hints at structural differences

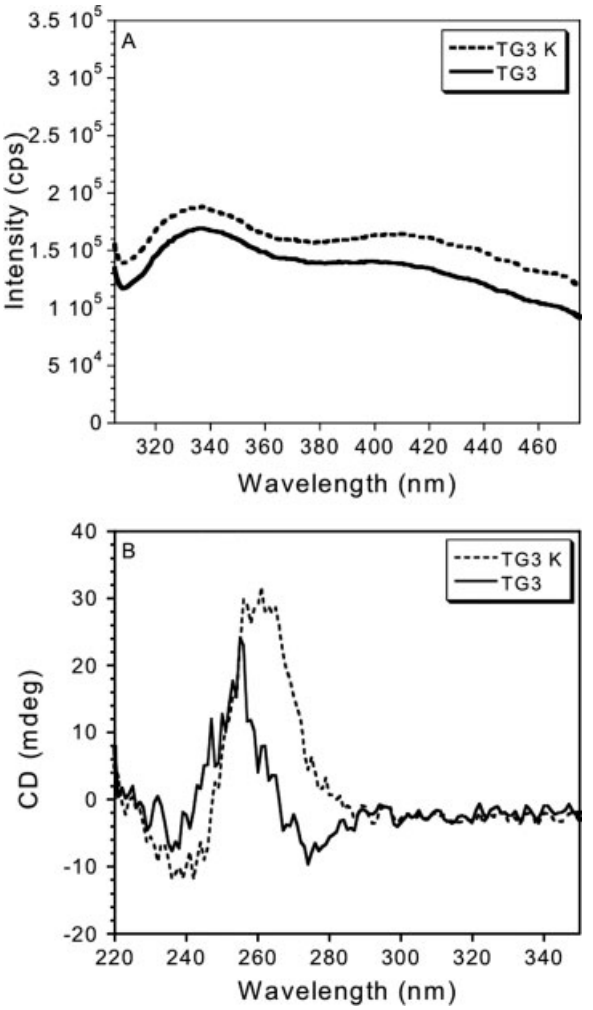

FIGURE 4 (A) Emission spectra of oligonucleotide TG3 in the presence (dotted line) and absence (solid line) of potassium ions. Each spectrum is the average of three independent spectra. (B) CD spectra of TG3 in the presence (dotted line) and absence (solid line) of potassium ions. The CD sample concentration was 67 μM and the emission sample concentration was 13 μM.

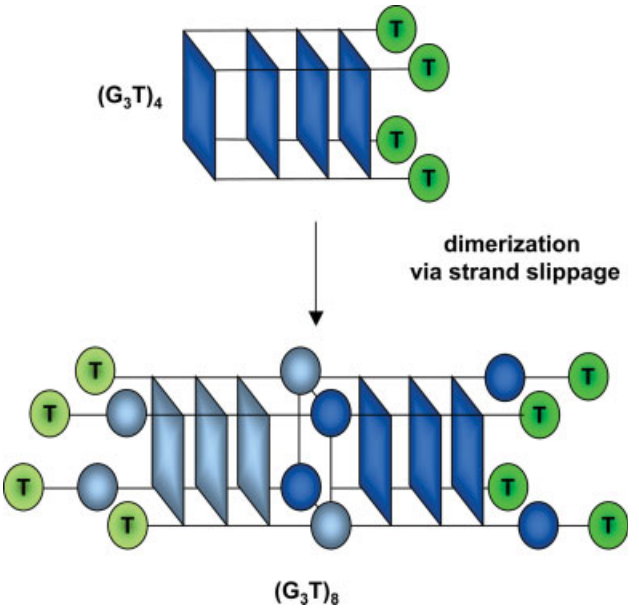

SCHEME 2 Proposed structures[22] of the quadruplexes formed by G_3T (top) and G_3T_{cyc} (bottom). The blue parallelogram represents a G-quartet plane; green circles are thymines; blue circles are guanines, the different shades (light and dark) indicate the two monomeric quadruplexes that have interlocked to create $(G_3T)_8$.

between the two sequences that CD spectroscopy does not provide.

Next, we applied the thermal cycling protocol of Krishnan-Ghosh et al. to both G3T and TG3. G3T forms an interlocked quadruplex upon thermal cycling (Scheme 2), but structures formed by TG3 have not been investigated. After cycling in the presence of potassium, both sequences produce emission spectra similar in shape and intensity (Figures 5 and 6). The CD spectra of $G3T_{cyc}$ and $TG3_{cyc}$ are consistent with formation of parallel-stranded quadruplexes (Figure S5). The emission spectra of $G3T_{cyc}$ and $TG3_{cyc}$ are most similar to spectra observed for the quadruplexes formed by G7 or G10 (Figure 1), because they lack an obvious shoulder at 390 nm. The emission spectrum of $G3T_{cyc}$, which corresponds to a majority of the "interlocked" species in solution on the basis of our PAGE results (vide infra) and previous NMR characterization,[28] presents a maximum at ~335 nm. In comparison, the spectrum of $TG3_{cyc}$ presents a maximum at 330 nm. Both cycled species display emission spectra with higher intensities than spectra collected after the exact same samples were heated to 95°C and subsequently cooled rapidly. The spectra of the annealed samples also are broader. For $G3T_{cyc}$, the spectrum collected after annealing and then slow cooling is the same as that collected after a second annealing step followed by fast cooling.

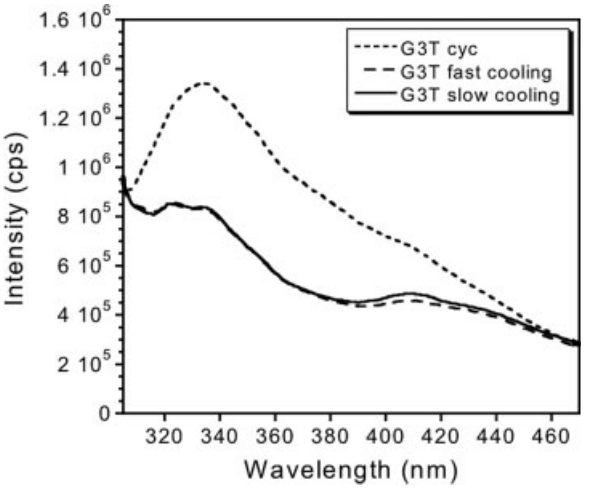

FIGURE 5 Emission spectrum of a sample of $G3T_{cyc}$ in buffer containing 10 m*M* KPi, 50 m*M* KCl, pH 7.0 (dotted line). Experiment was performed at room temperature, excitation at 270 nm. The strand concentration was 12 μM (absorbance of 0.15 in a 0.3 cm path length cuvette). The dashed line is a spectrum of the cycled sample after heating to 95°C, rapid cooling on ice, and equilibration to 4°C for 24 h. The solid line is a spectrum of the same sample after heating to 95°C, slow cooling over 3 h, and equilibration to 4°C for 24 h.

In contrast, $TG3_{cyc}$ displays a difference in intensity following the reannealing and cooling steps. The reheating and rapid or slow cooling protocol was designed to disrupt the inter-

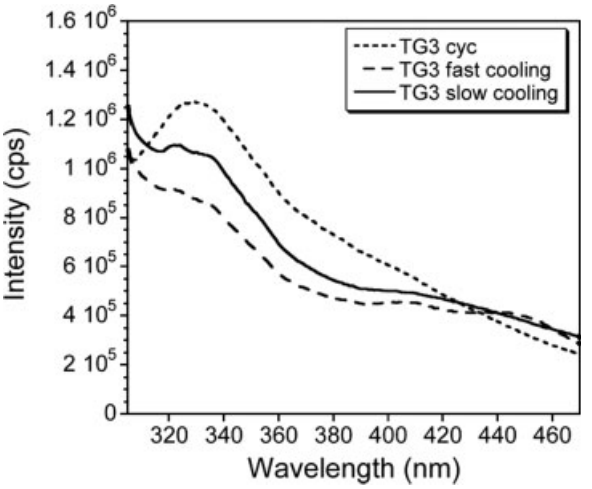

FIGURE 6 Emission spectrum of a sample of $TG3_{cyc}$ in buffer containing 10 m*M* KPi, 50 m*M* KCl, pH 7.0 (dotted line). Experiment was performed at room temperature, excitation at 270 nm. The strand concentration was 13 μM (absorbance of 0.15 in a 0.3 cm path length cuvette. The dashed line is a spectrum of the cycled sample after heating to 95°C, rapid cooling on ice, and equilibration to 4°C for 24 h. The solid line is a spectrum of the same sample after heating to 95°C, slow cooling over 3 h, and equilibration to 4°C for 24 h.

locked quadruplex species formed by G3T (and potentially TG3). The control sequence G4na has a much smaller emission intensity following thermal cycling than either G3T or TG3 (Figure S6). To further explore the structures formed by TG3 and G3T with and without thermal cycling, native polyacrylamide gel electrophoresis (PAGE) was employed.

Gel Electrophoresis

Another way to analyze quadruplex structures is by PAGE. This method separates species on the basis of size and is sensitive to the shape and surface charge of the analytes being separated. When thermally cycled G3T and TG3 oligonucleotides are analyzed by 16% nondenaturing PAGE, we observe two bands for each oligonucleotide (Figure 7). One band migrates slightly more quickly in the gel than the single-stranded 12-mer control G4na. A second species migrates more slowly. For both oligonucleotides, the fraction of the total sample that migrates more slowly increases upon thermal cycling of the samples. This observation obtains particularly for G3T (compare lanes 1 and 2). The "slow" species migrates more slowly for TG3 than for G3T (compare lanes 2 and 4). The relative mobility of the different species was confirmed using several molecular weight standards: 4-mer, 12-mer, and 24-mer oligonucleotides (Supporting Figure S7).

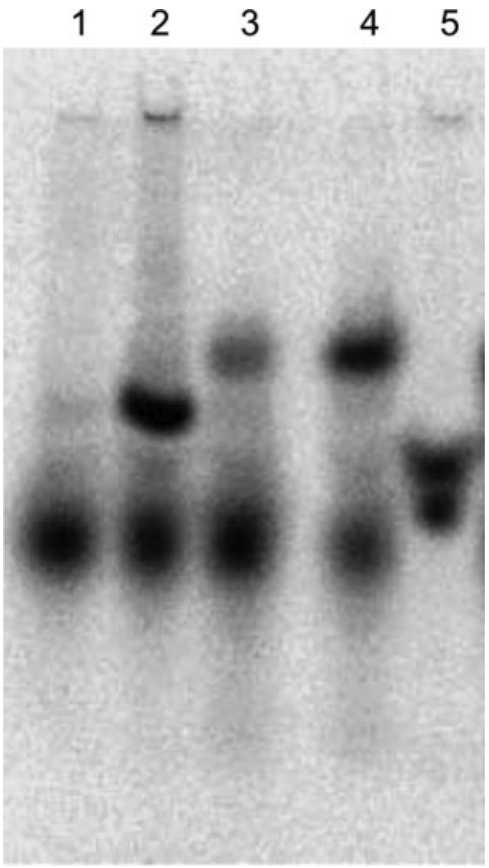

FIGURE 7 Nondenaturing PAGE of TG3 and G3T sequences prepared with or without cycled annealing. All samples contain potassium. Lane 1, G3T; lane 2, $G3T_{cyc}$; lane 3, TG3; lane 4, $TG3_{cyc}$; lane 5, G4na and G7na (molecular weight standards). The 16% gel containing 20 m*M* KCl was run for 3 h at 500 V in 0.5× TBE that also contained 20 m*M* KCl.

DISCUSSION

We found that the emission intensity of small, unmodified oligonucleotides rich in Gs varies depending on the distribution of guanines in the strand (contiguous vs. random distribution). G-rich sequences with contiguous guanines present significantly different intensities from homologous sequences containing interspersed Gs.[26,27] The general trends in the fluorescence spectra observed in our work are that (1) the fluorescence maximum wavelength is approximately the same in all of the spectra collected in the presence of K^+ and (2) some oligonucleotides present an additional shoulder at 390–395 nm in the presence of K^+.

As the G content increases, the steady-state emission intensity is expected to increase on the basis of previous measurements reporting increasing fluorescence quantum yields and lifetimes as a function of G content: 0.8×10^{-4} for GMP, 1.3×10^{-4} for GpG, and 4.7×10^{-4} for polyG.[1,23,26,27] We obtain a quantum yield for the G9 quadruplex of 2.4×10^{-4}, which is between the values for GpG and poly(G). The quantum yield is not a simple linear function of the number of guanines in the sequence, which we attribute to structural differences.[23,24,26,27] GMP is monomeric in solution, whereas G9 and poly(G) adopt tetrastranded structures.[35] Quadruplex formation has been hypothesized to affect excited-state lifetimes on the basis of work with a polyG sequence containing 20 guanines[27] which is similar to a sequence containing 20 contiguous Gs flanked by thymine residues forms a quadruplex in sodium-containing buffer.[36] Additional quantum yield (and other photophysical) measurements on quadruplexes will be required to reveal the effects of guanine content and structure on the intrinsic fluorescence.

The importance of subtle environmental and sequence effects in quadruplexes is illustrated by comparison of 4G and G4. The emission intensity per quadruplex for 4G (2.7×10^6 cps/μM quadruplex) in K^+ is much larger than that for G4 (1.8×10^6 cps/μM quadruplex) with K^+. Both sequences contain quadruplexes with four guanines (i.e., four guanine quartets), but the emission intensities vary significantly. In fact, the emission intensity per quadruplex for 4G is the same as that of the longer quadruplex G9 (2.7×10^6 cps/μM quadruplex). One explanation for this result is

that 4G forms longer species via quadruplex-stacking. Quadruplex stacking has been observed in crystal structures of quadruplex sequences with three or four guanines that also contain flanking bases.[31,37–39] Such stacking will protect more guanines from water, preventing solvent mediated quenching pathways (dynamic quenching).

Another factor to consider is the dynamic nature of G-rich oligonucleotides involving equilibration between single stranded and quadruplex structural forms. For G4 and G7, our previous mass spectrometry and gel electrophoresis data[33] indicate that the equilibrium almost completely favors the G-quadruplex form (>95%). A small amount of single-stranded oligonucleotide is observed, however, indicating that single-stranded oligonucleotide fluorescence contributes. We would argue, however, that the majority of the fluorescence we observe is due to quadruplexed, rather than single-stranded, oligonucleotide on the basis of our experiments in TMAC vs. potassium-containing solutions.

To further investigate the impact of an increasing number of quadruplex stacks on fluorescence intensity using the same sequence, we used the oligonucleotide G3T. This sequence forms a simple "monomeric" quadruplex composed of four strands and an "interlocked" species assembled from eight strands (Scheme 2). Using this sequence tests if there is a correlation between emission intensity and quadruplex extent (i.e., the number of quartet stacks in the quadruplex). As expected based on our results with the oligonucleotides G4, G7, and G9, we observe differences in the emission spectra of G3T in its monomeric (G3T with K^+) and interlocked ($G3T_{cyc}$ with K^+) quadruplex forms. We speculate that the differences observed in the emission spectra are due to changes in the stacking interactions in these different structures plus the contribution of more Gs being protected from solvent in the interlocked form. Furthermore, we probed the structurally uncharacterized sequence TG3. For TG3, we observe very similar emission spectra following thermal cycling that are consistent with the idea that TG3 forms two quadruplex-containing species with or without thermal cycling. These results suggest that emission spectroscopy correlates with structure and can differentiate the effects of the different temperature treatments. The features of the emission spectra as well as CD suggest that TG3 forms a larger structure than a monomeric G-quadruplex, possibly with similar geometry, but not identical to, the interlocked quadruplex formed by G3T.

On the basis of the native PAGE results, $G3T_{cyc}$ and $TG3_{cyc}$ both form monomeric quadruplex and an interlocked or extended quadruplex structure that migrates slowly. The monomeric quadruplex is expected to run faster than a single-stranded 12-mer because the quadruplex is structurally more compact. The decreased mobility of the slowly migrating species for $TG3_{cyc}$ compared with $G3T_{cyc}$ could be either because the species has a larger molecular weight—which seems unlikely—or because the structure is different. A structural difference also can explain why the emission spectra of these two thermally cycled oligonucleotides are different.

The exact reason for the enhanced fluorescence observed for quadruplex-forming oligonucleotides is not absolutely clear because current understanding of the excited states and electronic properties of complex macromolecules like DNA is incomplete.[23] The emission of DNA in its polymeric form has been attributed to excimers that give rise to broad, featureless spectra like those we observe.[23,40] We, therefore, speculate that the main contributor to the emission observed for our samples is a $^1G^*G$ excimer. On the basis of this assignment, the sequence, base-stacking, and structural heterogeneity for each quadruplex structure is expected to impact the excited-state and energy transfer properties of the system with effects, ultimately, on the intensity of the steady-state fluorescence spectrum.

There are several observations that show the importance of base stacking for energy transfer between bases and its effect on the DNA emission profile.[1,23,24,26,27] Singlet energy transfer between bases has been observed for photo-induced electron transfer between guanine and 2-aminopurine (2AP), a fluorescent analog of guanosine and adenosine, and between guanine and 1,N6 ethenoadenine.[41] In that case, it was hypothesized that quenching of the fluorescent nucleotide (2AP or 1,N6-ethenoadenine) depends on the extent of stacking interaction of the fluorescent probe with flanking bases. These authors observed that 1,N6 ethenoadenine was not quenched as readily as 2AP, which was attributed to a lower stacking interaction of 1,N6 ethenoadenine with G. Another group found that energy transfer from bases to 2AP was increased at low temperature.[42] This phenomenon occurs because decreasing the temperature reduces DNA motion, and maximizes stacking interactions. These authors observed that the sequence (GGGG[2AP]GGGG) displayed the least temperature-dependent change in the intensity of the 2AP excitation peak, which was explained as being due to nonstacking electronic interactions. We propose, however, that the lack of temperature dependence of the energy transfer between G and 2AP could be explained if the sequence in question forms a quadruplex, which is already somewhat rigid. If the sequence forms a quadruplex, decreasing the temperature should not change stacking interactions as much as for the other single-stranded sequences investigated.[42] Our observations could thus be explained by increased stacking favoring the formation of emissive static excimer-like species that is increased when several Gs are

together without interrupting bases to block singlet energy transfer.

In summary, we have shown that the emission intensity of G-rich sequences with contiguous Gs is higher than for single-stranded and double-stranded sequences lacking consecutive Gs. This observation allows us to monitor G-quadruplex structure using emission spectroscopy and reveal differences in the solution superstructure that cannot be easily detected by UV absorbance or CD spectroscopy. As a result, we envisage that emission can be used to characterize other systems where use of unmodified oligonucleotides is critical to conserve the native structure of G quadruplexes, in particular, under conditions where supramolecular structure formation is mediated by quadruplex stacking interactions. In addition to further work to determine contributions to the fluorescence intensity, we are exploiting the emission properties of untagged G-quadruplexes to evaluate ligand binding.[43]

EXPERIMENTAL SECTION

Materials

All deoxyoligonucleotides were purchased from Midland Oligos (Midland, TX). Oligonucleotides were resuspended in MilliQ water (TOC = 34 ppb or less, Ω = 18.2 conductivity), ethanol precipitated using a previously reported protocol, and resuspended in MilliQ water.[33] Alternatively, very short oligonucleotides with fewer than five bases were directly resuspended in water without ethanol precipitation. The strand concentration was determined using a Jasco spectrophotometer V-560. The extinction coefficients for each sequence (given in Table I) were obtained by the nearest neighbor approximation method.[44] Tetramethylethylenediamine, ammonium persulfate, mercaptoethanol, magnesium chloride, potassium chloride, 2,5-diphenyloxazole (99%, scintillation grade), guanine (99+%), cyclohexane (spectrophotometric grade 99+%) were supplied by Acros (Morris Plains, NJ). Microcon centrifugal filter devices were purchased from Millipore Corporation (Bedford, MA). MicroSpin G-50 Columns were ordered from GE Healthcare (Amersham, UK). Solutions of 40% acrylamide–bisacrylamide in a 19:1 ratio were purchased from National Diagnostics (Atlanta, GA). Tris(hydroxymethyl)aminomethane (Tris), boric acid, monobasic and dibasic potassium phosphate were purchased from Fisher (Pittsburgh, PA).

Emission Spectroscopy

All emission spectra are the sum of three scans with an integration time of 0.5 s, an excitation and emission slit width of 5 nm, path length 0.3 cm, collected in the range from 300 to 480 nm. The excitation wavelength was 270 nm. The spectra were collected on a Jobin-Yvon-Spex Fluorolog 3-11 fluorimeter or a Fluoromax-3 fluorimeter. The instrument-specific photomultiplier tube correction file supplied by the manufacturer was applied to all spectra.

Table I Abbreviations, Sequences, and Extinction Coefficients of Deoxyoligonucleotides

Abbreviation	Sequence	Nearest Neighbor ε (mM^{-1} cm^{-1})
G4na	5′TTGTGTGTGATT3′	112.7
G7na	5′TGTGTGTGTGTGAGT3′	144.8
G9na	5′TGGTGTGTGTGATGTGTG3′	173.3
G4	5′TTTTGGGGTTTT3′	106.4
G7	5′TTTTGGGGGGGTTTT3′	136.7
G9	5′TTTTGGGGGGGGGTTTT3′	156.9
9G-1	5′GATGAGAGTTAGTGATGAGTG3′	222.7
9G-2	5′CACTCATCACTAACTCTCATC3′	190.2
G3T	5′GGGT3′	40.2
TG3	5′TGGG3′	39.2
4G	5′GGGG3′	41.8

For spectra of samples with potassium, oligonucleotides G4, G7, G9, G4na, G7na, G9na (30 μM strand concentration), and double-stranded DNA (9G-1:9G-2, 30.0 μM duplex concentration) were suspended in buffer containing 10 mM KP_i and 50 mM KCl, pH 7.0. The duplex contains the same number of guanines as the G9 oligonucleotide.

To test if a change in the supramolecular structure of G rich oligonucleotides has an effect on the emission spectra, we prepared matched oligonucleotide samples (G3T, TG3, 4G) with and without added potassium. G-quadruplex formation is favored in the presence of monovalent cations such as potassium.[6,45,46] Samples for emission spectroscopy had an absorbance of ~0.15 in a 0.3 cm path length cuvette. Samples were prepared either in 10 mM KPi, 50 mM KCl, pH 7.0, or in deionized water. CD spectra also were collected, but for these samples, the absorbance was 0.8 in a 0.3 cm path length cuvette. A total volume of 300 μL was used for each sample. Samples with and without added K^+ were heated to 90°C for 10 min. The sample with potassium was cooled to room temperature over ~3 h. The sample in water was placed on ice for 5 min and then stored at 4°C. This rapid-cooling procedure was used to minimize quadruplex formation. Both sets of samples were equilibrated to room temperature immediately before collection of the emission and CD spectra (vide infra). Samples were placed in a 0.3 cm quartz cuvette and emission spectra were collected with the parameters previously described. Spectra were collected in triplicate and multiple times for all samples.

Comparison of the Emission of Different G-Quadruplex Structures

Samples of the deoxyoligonucleotides G3T and TG3 were prepared using several protocols to induce different structures. The first method applied was temperature cycling. The interlocked quadruplex formed by G3T was prepared using the protocol described by Krishnan-Ghosh et al.[28] In brief, lyophilized deoxyoligonucleotide G3T was resuspended in buffer 10 mM KPi, 50 mM KCl, pH 7.0 to give a concentration of ~500 μM strand. The sample was heated at 55°C for 16 h, then cooled to 30°C, and reheated to 55°C three times at a rate of 0.5°C/min in a thermal cycler (Eppendorf Master-

cycler). Samples were cooled to 10°C at a rate of 0.5°C/min and equilibrated at 5°C for 24 h. The same protocol was applied to the TG3 oligonucleotide, the structure of which has not been examined following thermal cycling. The control oligonucleotide G4na, a sequence that does not form quadruplexes, also was submitted to the same procedure. Samples prepared by thermal cycling are labeled $G3T_{cyc}$, $TG3_{cyc}$, and $G4na_{cyc}$ throughout the text. For emission spectra, the stock solutions of $G3T_{cyc}$, $TG3_{cyc}$, and $G4na_{cyc}$ were diluted with the appropriate amount of buffer to give an absorbance of 0.15 in a 0.3 cm path length cuvette. The samples for emission spectroscopy were further subjected to two sequential procedures that were expected to change the suprastructure. Emission spectra were collected after each of the procedures. First, the samples were heated to 95°C, cooled slowly over 2 h, and equilibrated to 4°C for 24 h. Then, the same samples were heated to 95°C and cooled quickly by immersion on ice followed by equilibration at 4°C for 24 h before collection of the emission spectra.

Quantum Yield Measurements

The following protocol was followed to cross calibrate the standards and later to derive the quantum yield of G9. UV-vis absorbance spectra were collected of the solvent background (cyclohexane for 2,5-diphenyloxazole or water for guanine), and of the sample in a 1 cm path length cuvette. Due to the low concentrations of 2,5-diphenyloxazole required ensure that the emission intensity was within the linear range of the Jobin-Yvon-Spex Fluorolog 3-11 fluorimeter, the absorption spectrum of only the stock solution was measured. Samples for the quantum yield measurements were prepared by serial dilution of the stock to generate the low absorbances required. Cyclohexane was purged with nitrogen before dissolution of 2,5-diphenyloxazole. Guanine was directly dissolved in MilliQ water rather than buffer as a means to minimize external variables and to be able to cross compare our values with those reported by Danies and Hauswirth.[47] The fluorescence spectrum of at least three samples was collected at every concentration. All spectra were corrected using the correction file for the instrument, the solvent spectrum was subtracted, and an average of at least three spectra was used to calculate final values. Fluorescence spectra were integrated to obtain areas and a plot of integrated fluorescence intensity vs. absorbance was generated. Data were fit with linear least squares regression method, with the intercept fixed at 0, to obtain the gradient [Grad in Eq. (1)]. The quantum yield was estimated using the equation:

$$\varphi_X = \varphi_{ST}\left(\frac{Grad_X}{Grad_{ST}}\right)\left(\frac{\eta_X^2}{\eta_{ST}^2}\right) \quad (1)$$

where φ_X is the quantum yield of the unknown, φ_{ST} is the quantum yield of the standard, η_X and η_{ST} are the refractive indices of the solvents for the unknown (X) and standard (ST) samples, $Grad_X$ and $Grad_{ST}$ are the slopes of the integrated-fluorescence intensity vs. absorbance plots for the unknown and standard, in that order. We cross-calibrated the guanine to 2,5-diphenyloxazole and then did a reverse cross-calibration (i.e., 2,5-diphenyloxazole as the standard and guanine as the unknown). For the quantum yield spectral collection, the following parameters were used: excitation bandwidth 5 nm, emission bandwidth 5 nm (the same bandwidth was used for the absorbance spectra), integration time of 0.1 s. Samples were excited at 275.5 nm to match the conditions in Daniels and Hauswirth.[47] The quantum yield of G9 was measured in 10 mKPi, 50 m*M* KCl buffer, pH 7.2.

Circular Dichroism Spectroscopy

CD spectroscopy is a useful means to detect and characterize parallel vs. antiparallel quadruplexes.[48] CD spectra were collected at room temperature using a Jasco J-715 spectropolarimeter coupled to a Dell Optiplex GX110 personal computer for data collection. Quartz cuvettes with path lengths of 0.3 or 1.0 cm (Starna, Atascadero, CA) were used. Each spectrum is the average of three scans and the spectrum for the blank was subtracted from this average. The spectra were collected with the following conditions: response 0.5 s, bandwidth 1 nm, and speed 200 nm min^{-1}.

The concentration of stock solutions was verified spectrophotometrically before each experiment. Stock solutions were vortexed and then centrifuged at 15,000 rcf in an Eppendorf microcentrifuge for 5 s. The concentration of DNA in the supernatant was determined by UV absorption at 260 nm. This protocol was adopted because we noticed that the oligonucleotides G3T, TG3, and 4G tend to aggregate into insoluble species at high concentration. CD spectra of G3T, TG3, 4G, and G4na oligonucleotides prepared in water or in buffer with and without temperature cycling were collected. An appropriate amount of the lyophilized oligonucleotide that had been resuspended in MilliQ water was used to make samples for CD spectroscopy. Samples labeled "cyc" were prepared by combining the appropriate volume of the previously cycled oligonucleotide stock solution with 100 m*M* KPi, 500 m*M* KCl, pH 7.0 buffer, and MilliQ water to give the desired final concentration of DNA in water or in pH 7.0 buffer with final concentrations of 10 m*M* KPi, 50 m*M* KCl.

General ^{32}P-Radiolabeling and Polyacrylamide Gel Electrophoresis

Oligonucleotides were gel-purified and ^{32}P-radiolabeled with [γ-^{32}P] ATP (10 mCi mL^{-1}, PerkinElmer Life Sciences, Boston, MA) using T4 polynucleotide kinase (Invitrogen, Carlsbad, CA) as previously described.[49] The following changes were introduced in the ^{32}P labeling protocol to improve labeling efficiency of G-quadruplex-forming sequences. A volume of 1 μL of a 5 μM oligonucleotide solution was added to 2 μL modified forward reaction buffer (350 m*M* Tris-HCl (pH 7.6), 50 m*M* $MgCl_2$, 5 m*M* 2-mercaptoethanol), and 3 μL of MilliQ water. The sample was heated to 90°C for 5 min and chilled on ice for 5 min before addition of T4 polynucleotide kinase and γ-^{32}P-ATP. Samples were applied to a MicroSpin G-50 Column according to the manufacturer's directions and the filtrate (~50 μL) was ethanol precipitated by adding 10 μL of 5*M* ammonium acetate and 500 μL ethanol. After removal of the supernatant, oligonucleotide pellets were air dried—rather than dried in a speed-vacuum system—to aid resuspension in gel-loading buffer. The samples for gel electrophoresis were prepared by mixing ^{32}P-radiolabeled oligonucleotide with unlabeled oligonucleotide to give a final concentration of 500 μM strand. The noncycled controls were prepared by heating them to 90°C for 5 min and cooling them quickly to 4°C using the thermocycler. Cycled radiolabeled oligonucleotides were prepared by combining ^{32}P-labeled oligonucleotide with unlabeled oligonucleotide to give a final concentration 500 μM strand and submitting the mixture to the temperature cycling

protocol described previously. Nondenaturing polyacrylamide gel electrophoresis (PAGE) was performed on 16% polyacrylamide gels containing 20 m*M* KCl and run in 0.5× Tris-borate-ethylenediaminetetraacetic acid (TBE) buffer containing 20 m*M* KCl.[33] TBE (10×) contains 0.89*M* Tris, 20 m*M* Na_2EDTA, and 0.89*M* boric acid, pH 8.3. Gel electrophoresis was performed at 4°C for 2–3 h at 500 V. Gels were wrapped in plastic wrap and placed on a phosphor screen, exposed from 30 min^{-1} h for quantification of band intensities, scanned on an Amersham Biosciences Typhoon 9200 instrument, and analyzed using Image QuaNT™ software. A slightly different protocol was used for ^{32}P-radiolabeling of oligonucleotide used for the gel in Figure S7. This protocol is described in the Supporting Information.

REFERENCES

1. Callis, P. R. Annu Rev Phys Chem 1983, 34, 329–357.
2. Kikin, O.; D'Antonio, L.; Bagga, P. S. Nucleic Acids Res 2006, 34, W676–W682.
3. Wieland, M.; Hartig, J. S. Chem Biol 2007, 14, 757–763.
4. Neidle, S.; Parkinson, G. N. Biochimie 2008, 90, 1184–1196.
5. Alberti, P.; Bourdoncle, A.; Sacca, B.; Lacroix, L.; Mergny, J.-L. Org Biomol Chem 2006, 4, 3383–3391.
6. Miyoshi, D.; Karimata, H.; Wang, Z.-M.; Koumoto, K.; Sugimoto, N. J Am Chem Soc 2007, 129, 5919–5925.
7. Kotlyar, A. B.; Borovok, N.; Molotsky, T.; Cohen, H.; Shapir, E.; Porath, D. Adv Mater 2005, 17, 1901–1905.
8. Kimura, T.; Kawai, K.; Fujitsuka, M.; Majima, T. Tetrahedron 2007, 63, 3585–3590.
9. Lakowicz, J. R.; Shen, B.; Gryczynski, Z.; D'Auria, S.; Gryczynski, I. Biochem Biophys Res Commun 2001, 286, 875–879.
10. Ramsay, G. Nat Biotechnol 1998, 16, 40–44.
11. Goel, G.; Kumar, A.; Puniya, A.; Chen, W.; Singh, K. J Appl Microbiol 2005, 99, 435–442.
12. Stojanovic, M. N.; de Prada, P.; Landry, D. W. J Am Chem Soc 2001, 123, 4928–4931.
13. Radi, A. E.; Acero Sanchez, J. L.; Baldrich, E.; O'Sullivan, C. K. J Am Chem Soc 2006, 128, 117–124.
14. Huang, W.; Tanaka, H.; Ogawa, T. J Phys Chem C 2008, 112, 11513–11526.
15. Wiederholt, K.; McLaughlin, L. W. Nucleic Acids Res 1999, 27, 2487–2493.
16. Green, J. J.; Ladame, S.; Ying, L.; Klenerman, D.; Balasubramanian, S. J Am Chem Soc 2006, 128, 9809–9812.
17. Ying, L.; Green, J. J.; Li, H.; Klenerman, D.; Balasubramanian, S. Proc Natl Acad Sci USA 2003, 100, 14629–14634.
18. Lu, M.; Guo, Q.; Kallenbach, N. R. Biochemistry 1992, 31, 2455–2459.
19. Green, J. J.; Ying, L.; Klenerman, D.; Balasubramanian, S. J Am Chem Soc 2003, 125, 3763–3767.
20. Markovitsi, D.; Gustavsson, T.; Sharonov, A. Photochem Photobiol 2004, 79, 526–530.
21. Lakowicz, J. R. Principles of Fluorescence; Kluwer Academic/Plenum: New York, 1999.
22. Mujumdar, R. B.; Ernst, L. A.; Mujumdar, S. R.; Lewis, C. J.; Waggoner, A. S. Bioconjug Chem 1993, 4, 105–111.
23. Crespo-Hernández, C. E.; Cohen, B.; Hare, P. M.; Kohler, B. Chem Rev 2004, 104, 1977–2019.
24. Crespo-Hernandez, C. E.; Kohler, B. J Phys Chem B 2004, 108, 11182–11188.
25. Markovitsi, D.; Sharonov, A.; Onidas, D.; Gustavsson, T. Chem Phys Chem 2003, 4, 303–305.
26. Crespo-Hernandez, C. E.; de La Harpe, K.; Kohler, B. J Am Chem Soc 2008, 130, 10844–10845.
27. Schwalb, N. K.; Temps, F. Science 2008, 322, 243–245.
28. Krishnan-Ghosh, Y.; Liu, D.; Balasubramanian, S. J Am Chem Soc 2004, 126, 11009–11016.
29. Stefl, R.; Cheatham, T. I.; Spackova, N.; Fadrna, E.; Berger, I.; Koca, J.; Sponer, J. Biophys J 2003, 85, 1787–1804.
30. Sen, D.; Gilbert, W. Nature 1988, 334, 364–366.
31. Phillips, K.; Dauter, Z.; Murchie, A. I. H.; Lilley, D. M. J.; Luisi, B. J Mol Biol 1997, 273, 171–182.
32. Aboul-ela, F.; Murchie, A. I.; Lilley, D. M. Nature 1992, 360, 280–282.
33. Evans, S. E.; Mendez, M. A.; Turner, K. B.; Keating, L. R.; Grimes, R. T.; Melchoir, S.; Szalai, V. A. J Biol Inorg Chem 2007, 12, 1235–1249.
34. Fasman, G. D. Circular Dichroism and the Conformational Analysis of Biomolecules; Plenum Press: New York, 1996.
35. Arnott, S.; Chandrasekaran, R.; Martilla, C. M. Biochem J 1974, 141, 537–543.
36. Ren, J.; Chaires, J. B. Biochemistry 1999, 38, 16067–16075.
37. Laughlan, G.; Murchie, A. I. H.; Norman, D. G.; Moore, M. H.; Moody, P. C. E.; Lilley, D. M. J.; Luisi, B. Science 1994, 265, 520–524.
38. Parkinson, G. N.; Lee, M. P. H.; Neidle, S. Nature 2002, 417, 876–880.
39. Parkinson, G. N.; Ghosh, R.; Neidle, S. Biochemistry 2007, 46, 2390–2397.
40. Eisinger, J.; Shulman, R. G. Science 1968, 161, 1311–1319.
41. Kelley, S. O.; Barton, J. K. Science 1999, 283, 375–381.
42. Xu, D.-G.; Nordlund, T. M. Biophys J 2000, 78, 1042–1050.
43. Mendez, M. A.; Szalai, V. A. Abstr Pap Am Chem Soc 2008, INOR-167.
44. Borer, P. N. In Handbook of Biochemistry and Molecular Biology; Fasman, G., Ed.; CRC Press: Cleveland, 1975; p 589.
45. Wang, Y.; Patel, D. J. Biochemistry 1992, 31, 8112–8119.
46. Gu, J.; Leszczynski, J. J Phys Chem A 2002, 106, 529–532.
47. Daniels, M.; Hauswirth, W. Science 1971, 171, 675–677.
48. Nagatoishi, S.; Tanaka, Y.; Tsumoto, K. Biochem Biophys Res Commun 2007, 352, 812–817.
49. Szalai, V. A.; Thorp, H. H. J Am Chem Soc 2000, 122, 4524–4525.

Reviewing Editor: Nils Walter